

SUPPLEMENTAL

Optimization of Electrospray Ionization Source Parameters for Lipidomics To Reduce Misannotation of In-Source Fragments as Precursor Ions

Rose M. Gathungu¹; Pablo Larrea^{1}; Matthew J. Sniatynski¹; Vasant R. Marur¹; John A. Bowden^{2,3}; Jeremy P. Koelme⁴; Pamela Starke-Reed^{5#}; Van S. Hubbard⁶; Bruce S. Kristal^{1&}*

¹Department of Medicine, Division of Sleep and Circadian Disorders, Brigham and Women's Hospital and Department of Medicine, Division of Sleep Medicine, Harvard Medical School, Boston, MA 02115

²Center for Environmental and Human Toxicology, Department of Physiological Sciences, College of Veterinary Medicine, University of Florida, Gainesville, FL, USA

³National Institute of Standards and Technology, Hollings Marine Laboratory, Charleston, SC 29412.

⁴Department of Pathology, Immunology, and Laboratory Medicine, College of Medicine, University of Florida, Gainesville, FL 32610.

⁵Deputy Director, NIH Division of Nutrition Research Coordination, Bethesda, MD 20892.

⁶Director, NIH Division of Nutrition Research Coordination, Bethesda, MD 20892

**Current Address:* AbbVie. Worcester, MA

#*Current Address: Deputy Administrator, Nutrition, Food Safety and Quality, Agricultural Research Service, USDA, Beltsville, Maryland 20705*

&CORRESPONDING AUTHOR: Email: bkristal@bwh.harvard.edu

Table of Content:

Supplemental Materials and Methods....**S-4**

Supplemental Results.... **S-6**

Supplemental Figure 1, Negative ion mass spectra in lipid extract with and without ISF... **S-6**

Supplemental Table 1, List of the most abundant lipids and fragment ions that can be misannotated... **S-7**

Supplemental Figure 2, Use of positive and negative ion analysis to resolve ISF.....**S-9**

Supplemental Table 2, Selected examples of overlap fragment and precursor ion masses within 2ppm.... **S-10**

Supplemental Table 3, Evaluation of relative quantitation of precursor ions that fragment in-source...**S-11**

Optimization of Source Parameters to Reduce ISF....**S-12**

Supplemental Figure 3, Skimmer Voltage and Tube Lens modulate ISF.....**S-13**

Supplemental Table 4, Effect on the ion count after tuning the ESI source with lipids from different classes... **S-15**

Supplemental Table 5, Examples of Lipids that Fragment In-source....**S-16**

Supplemental Materials and Methods:

Internal standard mixture: The internal standard mixture consisted of five lipids: PC(17:0/17:0) at 5 µg/mL, PG(15:0/15:0) at 5 µg/mL, PE(17:0/17:0) at 10 µg/mL, LPC(19:0/0:0) at 5 µg/mL, and PS(17:0/17:0) at 30 µg/mL.

Preparation of Lipid Standards: Preparation of stock lipid standards at concentrations ranging from (1-10 mg/ml) was achieved by dissolving them in DCM:MeOH(2:1,v/v). 1-nonadecanoyl-sn-glycero-3-phosphocholine (LPC (19:0)), 1,2 heptadecanoyl-sn-glycero-3-phosphoethanolamine (PE (17:0/17:0)), 1,2-dipentadecanoyl-sn-glycero-3-phospho-(1'-sn-glycerol) (PG 15:0/15:0), 1,2-diheptadecanoyl-sn-glycero-3-phosphocholine (PC 17:0/17:0), 1,2-diheptadecanoyl-sn-glycero-3-phosphoserine (PS 17:0/17:0), linoleic acid (FA (18:2)), oleic acid (FA ((18:1))), arachidonic acid (FA (20:4)), docosahexaenoic acid (FA(22:6)), palmitic acid (FA (16:0)), and stearic acid (FA(18:0)).

Lipid Extraction: Lipids were extracted from 30 µL of a human plasma pool which was first spiked with 30 µL of the internal standard mixture. Then, 180 µL of methanol was added to each sample and the sample vortexed for 20 s. 380 µL of DCM was then added followed by 20 s of vortexing. For phase separation, 120 µL of water was added to the sample, vortexed for 20 s and the sample allowed to sit at room temperature for 10 min. The lipid layer (bottom layer) was then pipetted out and the solvent dried down under vacuum. Prior to LC-MS analysis, the lipid extract was re-constituted in 300 µL ACN/IPA/H₂O (65:30:5 v/v/v) containing PG (17:0/17:0) at a concentration of 2.5 µg/mL.

LC-MS Analysis: Lipid extracts were separated on an Ascentis Express C18 2.1 x 150 mm 2.7 µm column (Sigma-Aldrich, St. Louis, MO). Separation was achieved on a binary solvent system whereby mobile phase A consisted of ACN:H₂O (60:40), 10 mM ammonium formate, 0.1% formic acid and mobile phase B consisted of IPA:ACN (90:10), 10 mM ammonium formate, 0.1% formic acid. A flow rate of 260 µL/min was used for the analysis and the column and sample tray were held constant at 55 °C and 4 °C, respectively.

MS Instrumentation

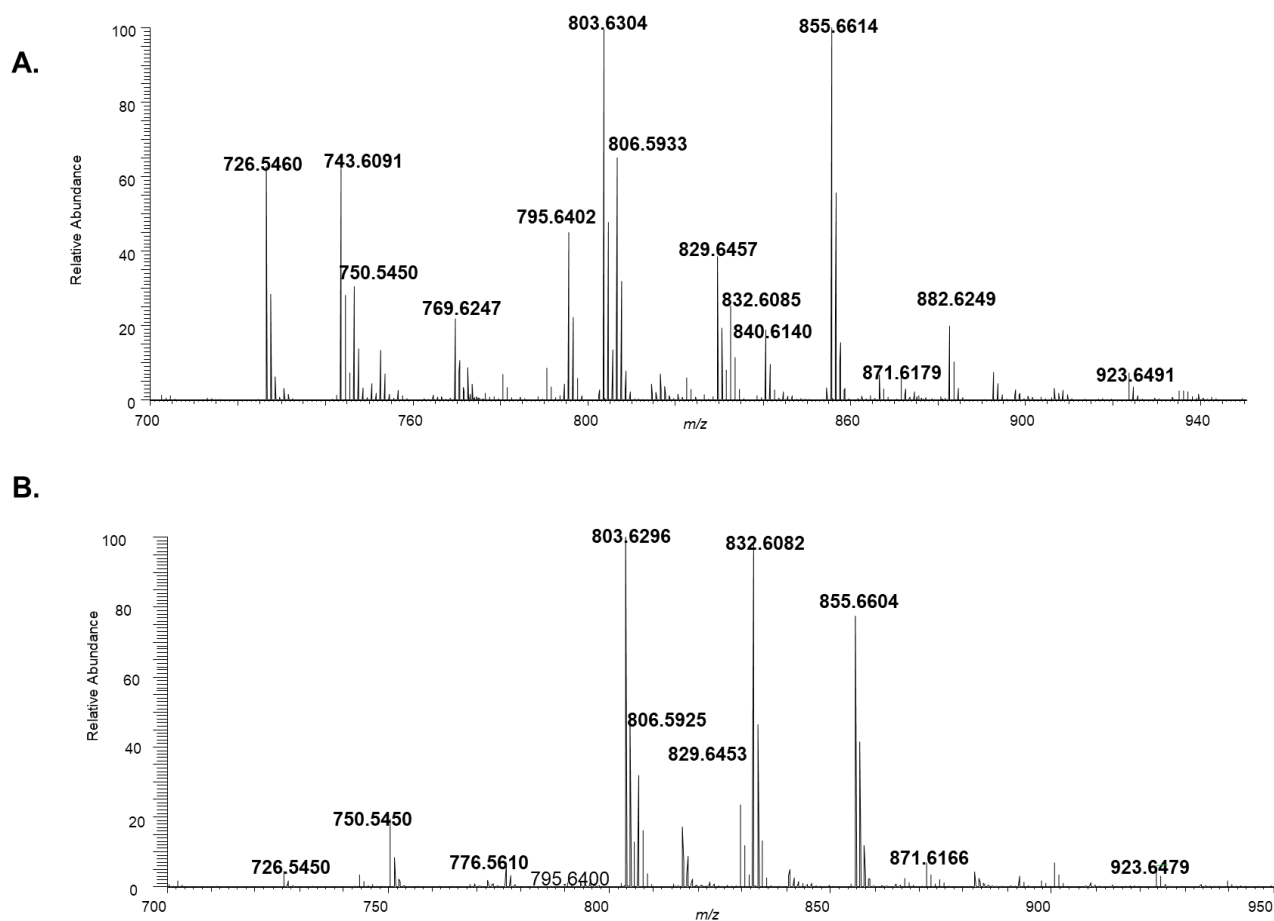
MS analysis was performed on an Exactive Benchtop Orbitrap Mass Spectrometer (Thermo Fisher, San Jose, CA) equipped with a heated electrospray ionization (HESI-II) probe. The HESI-II probe was run in the ESI mode (i.e., the HESI vaporizer temperature was off). In both the positive and negative ionization modes, the heated capillary (ion transfer tube) temperature was held at 280 °C, the sheath gas flow was set to 30 units and the auxiliary gas was set to 20 units. The spray voltage was set to 3.8 kV in the negative mode and 4 kV in the positive mode. Full scan MS spectra in the negative mode were acquired in the high-resolution mode (a resolution of 60k) and a 2 Hz scan speed

Direct Infusion of Lipids: To individually assess the source parameters that affected source fragmentation, LPC(19:0) was infused into the MS. The infusion was done by teeing in via a splitter 250 $\mu\text{l}/\text{min}$ of 50:50 mobile phase A: mobile phase B and 2.5 $\mu\text{g}/\text{ml}$ of LPC(19:0) flowing at 10 $\mu\text{l}/\text{min}$ for a total flow of 260 $\mu\text{l}/\text{min}$ into the MS to mimic the LC flow rate. The MS was tuned with PG(17:0/17:0) as previously reported.^{1,2} The MS was also tuned with LPC(19:0), PE(17:0/17:0) and PC(17:0/17:0) all at 2.5 $\mu\text{g}/$

SIEVE analysis: the framing parameters in the quantitation experiments were: 5 ppm for the m/z window, 1.00 minutes for the RT window, and masses between m/z 200 and 1500. The intensity threshold was set at 1000, with 10,000 frames selected. A plasma sample analyzed in the middle of the analysis was used as a reference.

Supplemental Results:

Supplemental Figure 1:



Supplemental Figure 1: Negative ion mass spectra of lipids in a plasma pool. The spectra are from the same chromatographic time point with **(A)** and without **(B)** In-Source Fragmentation.

- A.** A mass spectrum of SMs and PLs with the presence of in-source fragmentation (ISF). The spectrum shows multiple ions some of which are in-source fragments
- B.** A mass spectrum of SMs and PLs after elimination of ISF. ISF reduces spectra complexity.

Supplemental Table 1:

A.	<u>m/z</u>	<u>RT</u>	<u>Lipid ID</u>
	802.563	14.83	PC(34:2)
	830.5947	16.87	PC(36:2)
	804.5787	16.42	PC(34:1)
	749.5361	16.59	PG(34:0)
	826.5633	14.51	PC(36:4)
	854.5942	16.55	PC(38:4)
	828.5789	15.48	PC(36:3)
	693.4734	12.71	PG(30:0)
	850.5635	14.01	PC(38:6)
	747.5685	13.93	SM(d34:1)
	885.5529	14.44	PI(38:4)
	856.6106	17.45	PC(38:3)
	806.5948	18.31	PC(34:0)
	857.6786	20.32	SM(d42:2)
	832.6104	18.50	PC(36:1)
	855.6628	18.43	SM(d42:3)
	852.579	14.68	PC(38:5)
	878.5947	16.07	PC(40:6)
	859.6945	21.91	SM(d42:1)
	750.5475	18.08	PE(P-38:4) or PE(O-38:5)
	831.6636	20.46	SM(d40:1)
	722.5159	16.06	PE(P-36:4) Or PE(O-36:5)
	852.5787	15.43	PC(38:5)
	762.5106	14.54	PE(38:6)
	766.5422	17.11	PE(38:4)
	810.5687	15.48	PC(O-36:5) or PC(P-36:4)
	776.548	14.42	PC(32:1)
	828.5788	14.98	PC(36:3)
	829.6476	18.54	SM(d40:2)
	854.5948	16.03	PC(38:4)
	826.564	13.49	PC(36:4)
	824.5486	13.20	PC(36:5)
	880.61	16.64	PC(40:5)
	812.5845	15.90	PC(O-36:4) or PC(P-36:3)
	775.6002	16.11	SM(d36:1)
	838.5999	15.98	PC(O-38:5) or PC(P-38:4)
	748.5316	16.24	PE(P-38:5) or PE(O-38:6)
	742.5425	17.45	PE(36:2)
	861.5527	14.70	PI(36:2)
	746.5162	15.55	PE(P-38:6)
	803.6318	18.26	SM(d38:1)
	745.5533	12.19	SM(d34:2)
	857.679	20.82	SM(d42:2)
	845.679	21.33	SM(d41:1)
	786.5689	15.86	PC(O-34:3) or PC(P-34:2)
	540.3322	3.58	LPC(16:0)
	774.5473	17.49	PE(P40:6)
	828.5792	16.02	PC(36:3)
	880.6107	17.38	PC(40:5)
	726.5471	18.46	PE(P-36:2) or PE(o-36:3)
	714.5106	15.48	PE(34:2)
	648.6323	22.95	Cer(d42:1)
	882.6268	18.06	PC(40:4)
	850.5639	13.19	PC(38:6)
	801.6155	16.44	SM(d38:2)
	773.5848	14.33	SM(d36:2)
	887.5686	15.36	PI(38:3)
	738.5107	15.17	PE(36:4)
	840.6157	17.93	PC(O-38:4) or PC(P-38:3)
	788.5838	16.23	PC(O-34:2) or PC(P-34:1)
	840.579	15.64	PC(37:4)
	843.6633	19.71	SM(d41:2)
	698.5155	16.42	PE(P-34:2) or PE(O-34:3)
	838.6002	17.45	PC(O-38:5) or PC(P-38:4)
	800.5483	13.48	PC(34:3)
	857.5224	12.50	PI(36:4)
	568.3636	5.46	LPC(18:0)
	833.5219	12.75	PI(34:2)
	817.5245	16.59	PI(O-34:3) or PI(P-34:2)

B.

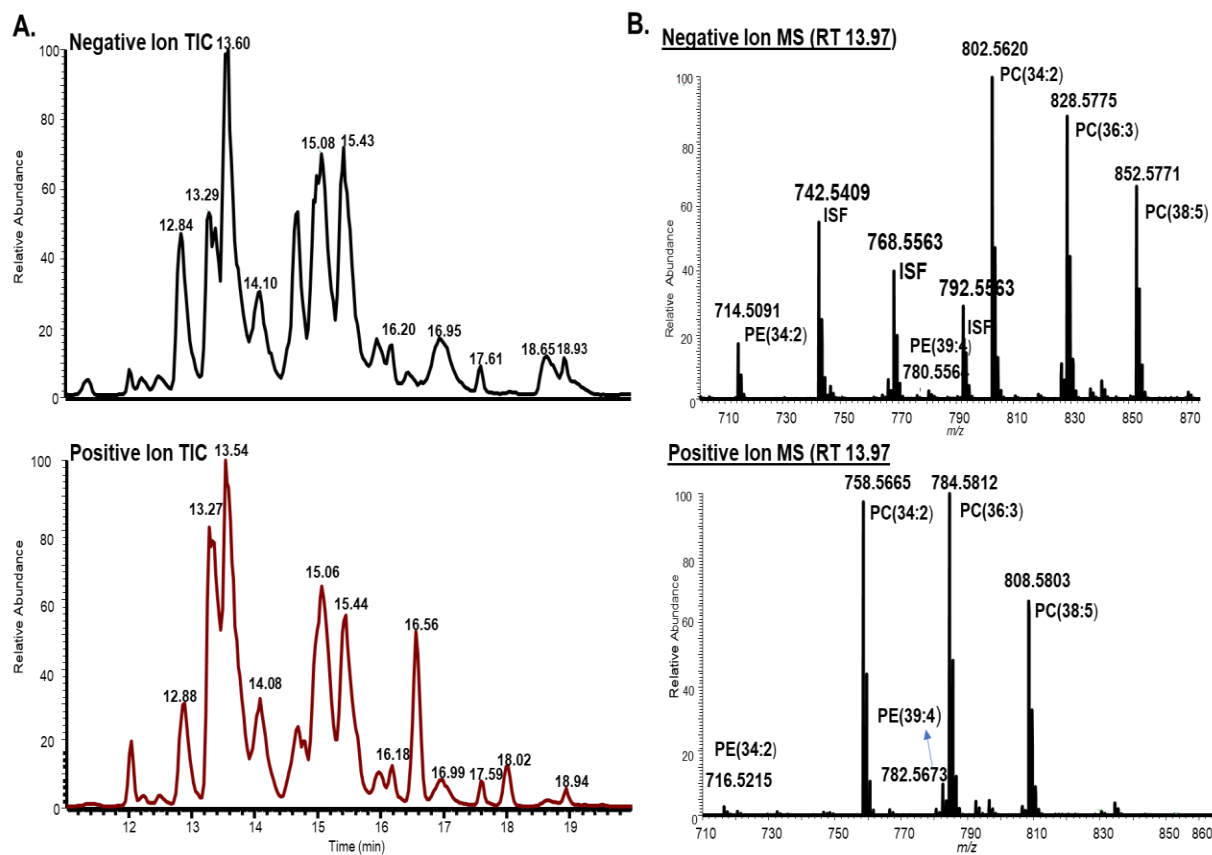
<u>m/z</u>	<u>RT</u>	<u>Source of Fragment</u>	<u>Misannotated As</u>
480.3109	3.56	LPC(16:0)	LPE(18:0)
508.3423	5.45	LPC(18:0)	LPE(20:0)
506.3267	3.89	LPC(18:1)	LPE(20:1)
504.3113	2.86	LPC(18:2)	LPE(20:2)
522.3579	6.44	LPC(19:0)	LPE(21:0)
718.542	16.26	PC(32:0)	PE(34:0)
716.5266	14.43	PC(32:1)	PE(34:1)
746.5737	18.31	PC(34:0)	PE(36:0)
744.5575	16.40	PC(34:1)	PE(36:1)
742.5418	14.82	PC(34:2)	PE(36:2)
742.5424	15.32	PC(34:2)	PE(36:2)
772.5893	18.50	PC(36:1)	PE(38:2)
770.5731	16.87	PC(36:2)	PE(38:2)
768.5578	14.98	PC(36:3)	PE(38:3)
768.5577	15.48	PC(36:3)	PE(38:3)
766.5423	13.49	PC(36:4)	PE(38:4)
766.5417	14.51	PC(36:4)	PE(38:4)
796.5896	17.44	PC(38:3)	PE(40:3)
794.5737	16.03	PC(38:4)	PE(40:4)
794.5734	16.54	PC(38:4)	PE(40:4)
792.5579	14.67	PC(38:5)	PE(40:5)
792.558	15.41	PC(38:5)	PE(40:5)
790.5423	14.01	PC(38:6)	PE(40:6)
820.5892	16.66	PC(40:5)	PE(42:5)
818.5737	16.07	PC(40:6)	PE(42:6)
726.5473	15.86	PC(O-34:3) or PC(P-34)	PE(P-36:2) or PE(O-36:3)
752.5628	15.87	PC(O-36:4) or PC(P-34)	PE(O38:4) or PE(P-38:3)
750.5471	15.48	PC(O-36:5) or PC(P-36)	PE(O-38:5) or PE(P-38:4)
778.5786	15.99	PC(O-38:5) or PC(P-38)	PE(P-40:5) or PE(O-40:4)
687.5467	13.95	SM(d34:1)	PE-Cer(d36:1)
685.5314	12.17	SM(d34:2)	PE-Cer(d36:2)
715.5784	16.13	SM(d36:1)	PE-Cer(d38:1)
713.5631	14.30	SM(d36:2)	PE-Cer(d38:2)
743.6106	18.25	SM(d38:1)	PE-Cer(d40:1)
741.595	16.42	SM(d38:2)	PE-Cer(d40:2)
771.6418	20.46	SM(d40:1)	no database hits
769.626	18.55	SM(d40:2)	no database hits
785.6574	21.32	SM(d41:1)	no database hits
799.6736	21.91	SM(d42:1)	no database hits
797.6575	20.32	SM(d42:2)	no database hits
797.6577	20.82	SM(d42:2)	no database hits

Supplemental Table 1:

A: The most abundant lipids in the MEC study arranged in order from the most abundant ion.

B: Fragment ions originating from PCs and SMs that can be misannotated as endogenous lipids.

Supplemental Figure 2:



Supplemental Figure 2: Use of both positive and negative ion mode helps resolve some in-source fragmentation issues

a: Positive and negative ion chromatograms (phospholipid and sphingomyelin region) of a lipid extract from a human plasma pool. The pool was analyzed by polarity switching between the positive and negative mode.

b: Negative (top panel) and positive (bottom panel) mass spectra of lipids eluting at 13.92 min. In the negative mode, multiple ions which included PCs, PEs and PC fragments were observed, by using the positive mode data, it was possible to distinguish which peaks represented endogenous lipids and which represented in-source fragments.

Supplemental Table 2:

Source of Fragment	Missannotated as	Fragment	<i>m/z</i>
Cer(d43:1)+H	CE(16:0)+NH ₄	NL H ₂ O	642.618
SM(d43:1)+H	CE(16:0)+NH ₄	NL PC(head)	642.618
GlcCer(d34:1)+H	Cer(d34:1)+H	NL C ₆ H ₁₀ O ₅	538.519
CerP(d34:1)+H	Cer(d34:1)+H	NL HPO ₃	538.519
SM(d38:0)+H	CerP(d40:1)+H	NL N(CH ₃) ₃	702.58
Sulfatide(d36:0)+H	DGTS(32:0)+H	NL H ₂ SO ₄	712.609
2OH-Sulfatide(40:1)	GlcCer(d34:2)+H	NL H ₂ SO ₄	698.557
DGTS(16:0_16:0)+H	LDGTS(16:0)+H	NL RCO+H (16:0)	474.379
PC(16:0_16:0)+H	LPC(16:0)+H	NL RCO+H (16:0)	496.34
PC(16:0_17:0)+H	LPE(20:0)+H	NL RCO+H (16:0)	510.355
LDGTS(42:0)+H	TG(O-49:2)+NH ₄	NL H ₂ O	820.775
PC(18:0_18:0)+H	LPC(P-18:1)+H	NL RCOOH+H (18:0)	506.361
SM(d24:0)+H	LPC(P-18:1)+H	NL N(CH ₃) ₃	506.361
PS(39:5)+Na	PS(P-34:0)+H	NL H ₃ PO ₄	748.549
Sulfatide(d18:1_16:0(2OH))+H	So(d16:1)+H	Amide(FA)+H	272.258
DGTS(48:0)+H	TG(55:2)+NH ₄	NL H ₂ O	918.849
Cer(d43:5)+H	zymosteryl(16:1)+NH ₄	NL H ₂ O	638.587
Ac2PIM2(36:2)-H	Ac2PIM1(36:2)-H	NL C ₆ H ₁₀ O ₅	1023.6
Ac3PIM2(16:0_18:1_18:1)-H	Ac2PIM2(36:2)-H	NL RCOOH+H (16:0)	1185.66
Deoxycholic acid-H	Dehydrolithocholic acid-H	NL H ₂ O	373.275
PC(38:6)+HCO ₂	DMPE(38:6)-H	NL CH ₃ +HCO ₂	790.539
PC(38:6)+C ₂ H ₃ O ₂	DMPE(38:6)-H	NL CH ₃ +C ₂ H ₃ O ₂	790.539
LPC(16:1)+C ₂ H ₃ O ₂	LPE(18:1)-H	NL CH ₃ +C ₂ H ₃ O ₂	478.294
LPC(16:1)+HCO ₂	LPE(18:1)-H	NL CH ₃ +HCO ₂	478.294
PC(16:1_16:1)+C ₂ H ₃ O ₂	LPE(18:1)-H	NL RCO-H+CH ₃ +C ₂ H ₃ O ₂	478.294
PC(16:1_16:1)+HCO ₂	LPE(18:1)-H	NL RCO-H+CH ₃ +HCO ₂	478.294
PE(18:1_18:1)-H	LPE(18:1)-H	NL RCO-H+serene	478.294
PI(16:0_16:0)-H	LPI(16:0)-H	NL RCO-H+serene	571.288
PC(32:4)+C ₂ H ₃ O ₂	PA(32:4)-H	NL choline+C ₂ H ₃ O ₂	639.403
PC(32:4)+HCO ₂	PA(32:4)-H	NL choline+HCO ₂	639.403
PG(32:4)-H	PA(32:4)-H	NL glycerol	639.403
PI(32:4)-H	PA(32:4)-H	NL inositol	639.403
PS(32:4)-H	PA(32:4)-H	NL serine	639.403
CL(18:2_18:3_18:3_20:4)-H	PA(36:4)-H	RCO-H(18:2)+RCO-H(16:0)+C ₃ H ₆ PO ₄	1667.435
PC(32:2)+C ₂ H ₃ O ₂	PE(34:2)-H	NL CH ₃ +C ₂ H ₃ O ₂	714.508
Ac2PIM1(36:2)-H	PI(36:2)-H	NL C ₆ H ₁₀ O ₅	861.55
2OH-Sulfatide(d36:2)	Sulfatide(d36:4)	NL H ₂ O	802.515

Supplemental Table 2:

Some selected examples of overlap of fragment and precursor ion masses within a 2 ppm mass accuracy window (plus or minus 1 ppm tolerance). Note that this table is not exhaustive, as tens of thousands of ions had overlapping fragments. "Source of fragment" shows a possible source of a fragment with the exact mass as a precursor ion. "Missannotated as" signifies a possible precursor which overlaps in *m/z*, and the *m/z* column is for the fragment ion. In all cases, one can deduce that numerous fragments and precursors from the respective classes overlapped in mass, although only one species is shown for illustrative purposes

Supplemental Table 3:

MZ	Time	Lipid ID	HHP 1	HHP 2	HHP 3	HHP 4	CV Day 1	HHP 5	HHP 6	HHP 7	HHP 8	CV Day 2
747.5662	12.99	SM(d18:1/16:0)	341191.49	354710.50	361536.63	327962.05	0.05	389803.67	367219.69	366849.70	355682.06	0.04
687.5449	13.00	Fragment of m/z 747	46220.71	48501.90	48975.69	43623.99	0.06	51824.46	49508.38	49744.39	49187.19	0.02
855.6598	17.00	SM(d18:2/24:1)	191416.50	214622.99	216933.05	156854.14	0.17	222998.53	200383.37	199610.89	195879.05	0.06
795.6395	17.00	Fragment of m/z 855	16285.07	18471.73	18392.13	13063.36	0.18	18949.34	17055.21	17112.36	16505.82	0.06
775.5979	14.88	SM(d18:1/18:0)	53210.80	54438.52	58959.07	46289.36	0.12	68129.17	59706.90	58173.24	56689.17	0.08
715.5765	14.88	Fragment of m/z 775	6013.66	6159.77	6594.65	5216.42	0.12	7621.89	6452.35	6504.47	6493.13	0.08
826.5607	13.46	PC(36:4)	991230.63	1037888.05	1098691.32	959614.06	0.07	1109940.53	975781.29	998364.71	943065.23	0.07
766.54	13.45	Fragment of PC (36:4)	71389.42	73280.57	77101.12	67055.75	0.07	76693.81	68492.51	68848.92	65832.03	0.07
854.5916	15.25	PC(38:4)	830038.78	868900.39	939813.64	759540.33	0.11	950014.38	837238.57	823369.76	810139.51	0.08
794.5712	15.25	Fragment of PC (38:4)	46968.04	49617.67	53451.84	42402.92	0.12	52878.26	46931.06	46675.37	45197.14	0.07
804.5761	15.13	PC(34:1)	1150912.35	1208343.74	1264894.45	1074822.64	0.08	1275691.56	1150192.97	1139777.82	1131750.59	0.06
744.5557	15.13	Fragment of PC(34:1)	78429.13	81165.13	84846.29	72023.06	0.08	84087.19	76232.25	76130.63	75606.38	0.05
540.3307	3.50	LPC(16:0)	182263.67	177119.04	174812.21	163372.92	0.06	183690.99	181265.28	174815.53	168830.84	0.04
480.3097	3.49	Fragment of LPC (16:0)	48441.43	47907.06	47455.33	43719.13	0.06	49518.68	49698.10	47194.79	45780.48	0.04
255.233	3.50	Fragment of LPC (16:0)	6266.65	6225.32	6097.42	5702.44	0.05	6412.07	6335.98	6175.94	5905.32	0.04
564.3306	2.81	LPC(18:2)	72353.56	69767.74	69796.79	65464.69	0.05	75025.94	73116.00	69910.76	66822.55	0.05
504.3101	2.81	Fragment of LPC (18:2)	18318.11	17754.11	17808.14	16457.20	0.06	18899.72	18663.39	18124.15	17080.32	0.04
279.233	2.81	Fragment of LPC (18:2)	3083.37	2982.50	2971.39	2757.15	0.06	3175.29	3114.52	3072.21	2852.05	0.05
MZ	Time	Lipid ID	HHP 9	HHP 10	HHP 11	HHP 12	CV Day 3	HHP 13	HHP 14	HHP 15	HHP 16	CV Day 4
747.5662	12.99	SM(d18:1/16:0)	404342.59	395175.80	388915.14	370723.19	0.04	480143.84	464265.07	451727.09	438195.27	0.04
687.5449	13.00	Fragment of m/z 747	52463.58	52458.74	50576.29	48178.96	0.04	63650.25	60574.46	58653.34	57228.76	0.05
855.6598	17.00	SM(d18:2/24:1)	218609.47	211174.97	229601.49	192843.73	0.07	245915.11	238118.52	225833.78	218122.81	0.05
795.6395	17.00	Fragment of m/z 855	17942.49	17301.09	18832.45	15760.13	0.07	20604.87	19519.03	18618.12	17742.59	0.06
775.5979	14.88	SM(d18:1/18:0)	67880.54	65009.63	68653.35	59054.89	0.07	77431.90	74659.28	70931.14	66694.37	0.06
715.5765	14.88	Fragment of m/z 775	7231.58	6941.60	7518.50	6439.63	0.07	8328.74	7995.47	7834.52	7268.61	0.06
826.5607	13.46	PC(36:4)	1053683.90	1001432.18	1034038.64	940284.84	0.05	1202445.09	1153886.30	1128461.48	1084361.04	0.04
766.54	13.45	Fragment of PC (36:4)	70307.08	66131.19	69253.62	62503.42	0.05	82942.57	77684.85	74558.35	72428.07	0.06
854.5916	15.25	PC(38:4)	879543.52	856147.39	931293.39	807205.39	0.06	1022916.73	1024931.94	977006.83	929870.58	0.05
794.5712	15.25	Fragment of PC (38:4)	46374.69	46328.91	50632.61	43834.77	0.06	55480.95	55350.66	51940.26	50056.77	0.05
804.5761	15.13	PC(34:1)	1212000.29	1177498.54	1248232.34	1106319.30	0.05	1412086.21	1414955.10	1358323.21	1289793.62	0.04
744.5557	15.13	Fragment of PC(34:1)	74666.81	75646.19	80019.17	71091.91	0.05	89056.41	89716.15	86721.43	81755.25	0.04
540.3307	3.50	LPC(16:0)	196498.23	192238.26	186749.43	175473.51	0.05	228310.72	219699.50	214798.78	202464.15	0.05
480.3097	3.49	Fragment of LPC (16:0)	51160.79	50066.93	48905.11	45195.08	0.05	61845.42	58822.04	57070.73	54199.74	0.06
255.233	3.50	Fragment of LPC (16:0)	6496.69	6471.33	6276.18	5778.48	0.05	7877.48	7469.50	7325.53	6954.99	0.05
564.3306	2.81	LPC(18:2)	80490.06	78820.32	76696.80	70612.15	0.06	94325.11	90785.38	88542.82	83391.04	0.05
504.3101	2.81	Fragment of LPC (18:2)	19558.70	19139.59	18792.12	17239.06	0.05	23281.88	22818.24	21747.97	20582.04	0.05
279.233	2.81	Fragment of LPC (18:2)	3240.44	3246.91	3133.40	2920.98	0.05	4029.40	3877.71	3737.12	3530.23	0.06
MZ	Time	Lipid ID	HHP 17	HHP 18	HHP 19	HHP 20	CV Day 5	HHP 21	HHP 22	HHP 23	HHP 24	CV Day 6
747.5662	12.99	SM(d18:1/16:0)	451787.77	483568.69	439949.30	435214.48	0.05	475915.87	450988.86	457695.57	450754.23	0.03
687.5449	13.00	Fragment of m/z 747	56960.59	61178.67	56114.95	55496.98	0.04	62031.27	59091.49	59352.04	58718.01	0.03
855.6598	17.00	SM(d18:2/24:1)	264057.73	261493.99	253890.02	243344.03	0.04	240442.62	246622.53	262656.17	244157.84	0.04
795.6395	17.00	Fragment of m/z 855	21079.25	21078.17	20476.21	19789.98	0.03	19849.29	20412.89	21906.45	20370.55	0.04
775.5979	14.88	SM(d18:1/18:0)	69897.26	75315.23	71100.40	68045.75	0.04	71896.18	68053.26	75474.92	70806.49	0.04
715.5765	14.88	Fragment of m/z 775	7309.25	8156.70	7406.96	7283.65	0.06	7768.53	7400.17	8245.86	8016.72	0.05
826.5607	13.46	PC(36:4)	1209562.45	1340646.23	1218013.36	1203730.71	0.05	1187738.03	1175039.28	1257178.65	1215114.85	0.03
766.54	13.45	Fragment of PC (36:4)	79988.56	88243.27	80220.56	78859.31	0.05	79841.33	79729.40	85253.34	80921.32	0.03
854.5916	15.25	PC(38:4)	1041761.34	1130168.56	1094807.63	1051580.65	0.04	1054755.65	1024006.81	1135676.44	1060409.00	0.04
794.5712	15.25	Fragment of PC (38:4)	54629.88	59567.12	57943.57	55356.29	0.04	56864.88	55394.28	60742.64	56159.90	0.04
804.5761	15.13	PC(34:1)	1452317.11	1534849.29	1491748.03	1440016.99	0.03	1458264.81	1415725.78	1529101.33	1451645.42	0.03
744.5557	15.13	Fragment of PC(34:1)	90913.93	95570.43	93703.76	89115.58	0.03	92446.38	88406.85	97647.16	92462.26	0.04
540.3307	3.50	LPC(16:0)	220745.37	219286.24	212221.13	200792.86	0.04	231580.15	224552.85	215417.30	205773.85	0.05
480.3097	3.49	Fragment of LPC (16:0)	57441.71	57223.49	55029.42	52539.37	0.04	62116.31	60573.16	57736.01	55583.10	0.05
255.233	3.50	Fragment of LPC (16:0)	7261.61	7188.09	6924.85	6556.87	0.05	7911.24	7717.01	7422.63	6991.44	0.05
564.3306	2.81	LPC(18:2)	89983.81	88819.37	86719.40	82446.41	0.04	94949.07	92791.91	89212.93	85273.07	0.05
504.3101	2.81	Fragment of LPC (18:2)	21864.56	21373.01	20996.84	20060.09	0.04	23648.22	23015.33	22434.09	21311.17	0.04
279.233	2.81	Fragment of LPC (18:2)	3706.65	3723.66	3599.15	3451.57	0.03	4019.65	3977.21	3808.08	3641.87	0.04

Supplemental Table 3: Inter and Intra-day evaluation of relative quantitative results of select lipids that fragment in-source. CVs are based on raw peak areas without normalization.

Optimizing Source Parameters to Reduce In-Source Fragmentation:

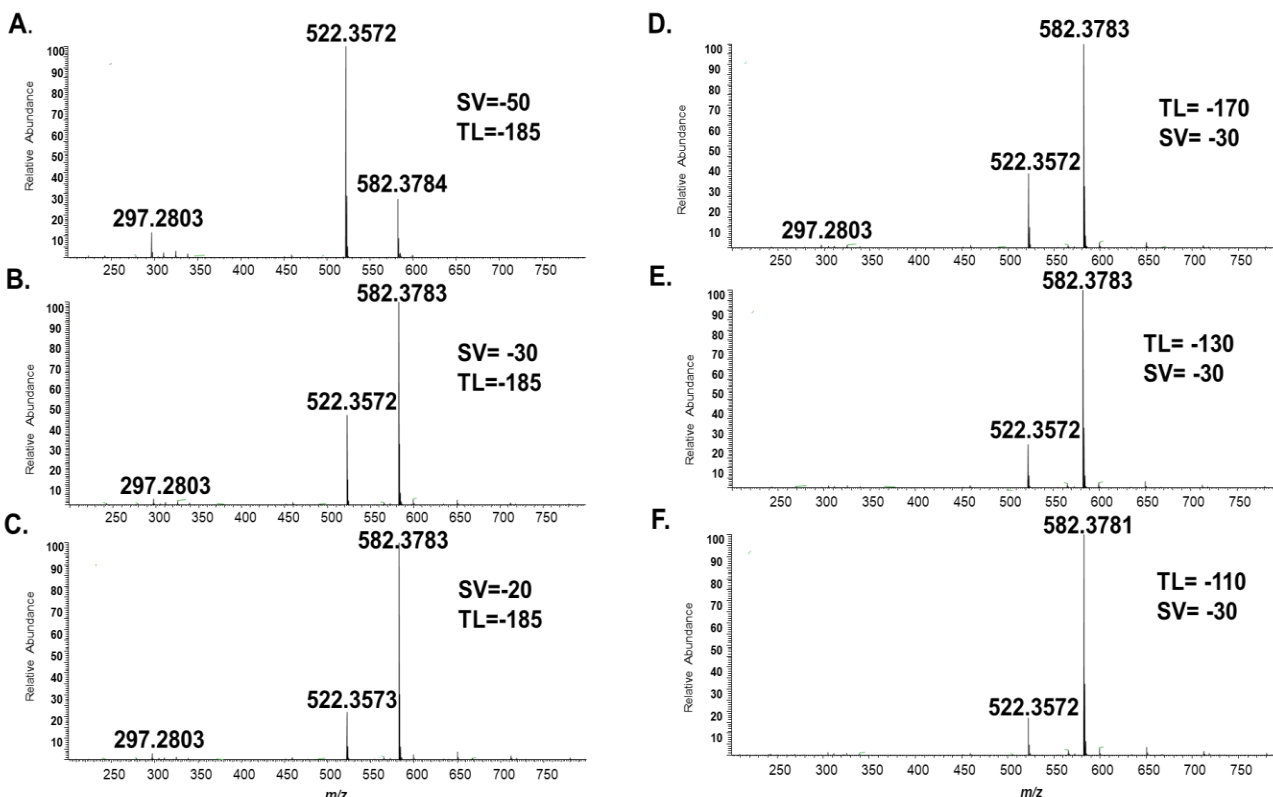
We assessed whether the ESI source parameters could be optimized to reduce ISF for the choline containing lipids. We were interested in finding a balance between reducing ISF while at the same time having complete desolvation of the mobile phase and having optimal ion transmission. For any given MS experiment, source parameters are usually optimized (through tuning) to i) ensure optimal transmission of ions to the mass analyzer and ii) to ensure complete desolvation of the mobile phase³. These source parameters include: i) the heated capillary temperature; ii) the drying gas flow rate (which is dependent on the LC flow rate); iii) the capillary voltage (CVT); iv) the tube lens voltage offset (TL), and v) the skimmer voltage (SV). These five parameters were examined to determine their effects on ISF. We first established that the heated capillary temperature (which if too high can lead to thermal decomposition of compounds) and the drying gas flow rate did not lead to ISF in our system (details in the supplemental section). Therefore, we aimed to evaluate the other source parameters, i.e., CVT, TL and SV.

We evaluated these parameters in two ways: i) manually, which allowed for a systematic evaluation of the effect of each source parameter on ISF, and ii) automatically, wherein we evaluated the extent to which tuning the MS using phospholipids differing in their head-group resulted in MS source settings that balanced high sensitivity detection of all lipids with minimal ISF. The automatic approach intrinsically adapts all source parameters simultaneously, and thus complements the manual, parameter by parameter approach. The automatic approach is also beneficial in that, long-term, it facilitates automating source settings and facilitates promulgation of this approach.

In the manual assessment, two of the three source parameters (i.e., CVT, TL, and SV) were kept constant, while the third source parameter was systematically manipulated. A LPC standard (LPC(19:0)) was used for this evaluation. The CVT did not have an effect on ISF and the ion intensity stayed the same regardless of the CVT applied (data not shown). Manipulation of the SV and TL both affected ISF as noted by the intensity of the molecular and fragment ions (Supplemental **Figure 3A-F**). At a high SV (e.g., SV=50V, the highest setting), the molecular ion (m/z 582; $[M+FA-H]^+$) was at a lower intensity than the in-source fragment ion (m/z 522 [i.e., $M-15$]⁺, which would unsuitably match LPE (21:0) in a database search, see **Figure 3A**). A second fragment ion (m/z 297, which would match FFA (19:0) from LPC(19:0), was also observed, but at a lower intensity than either the molecular ion or the m/z 522 fragment ion. Thus, under inappropriate source parameters, LPC (19:0) can be misinterpreted as at least two other lipids.

As the SV was reduced, the intensity of the molecular ion increased and at a 20V potential, the intensity of the fragment ion at m/z 522 dropped to below 20% of the molecular ion (**Figure 3B and C**). Note that when the SV was dropped to 5V (**data not shown**), the intensity of the molecular ion also dropped. The results indicated that an SV of between 20-30V was optimal for observation of the lowest intensity of the m/z 522 fragment ion, while maintaining the intensity of the molecular ion.

In similar experiments, reducing the TL voltage was found to primarily reduce the level of the FFA in-source fragment derived from LPC 19:0 (**Figures 5D-5F**).



Supplemental Figure 3: SV and TL modulate in-source fragmentation

a-c: ISF as a function of SV. The intensity of the molecular ion of LPC(19:0) vs. the in-source fragments increased as the SV was reduced. All other source parameters were kept constant. **d-f:** ISF as a function of tube lens voltage with the SV kept constant at 30V. Intensity of the in-source fragments of LPC(19:0) further reduced with a reduction in the tube lens voltage in the negative ionization mode.

After establishing that TL and SV had the most effect on ISF, we next assessed the use of a specific PL to auto-tune the source. When analyzing complex lipidomics samples, it is important to tune using a lipid that ensures optimal detection of all lipids in a mixture. The choice of lipid is critical, as the lipid head group and FA chain composition can potentially change source parameters affecting the transmission of lipids and extent of ISF. In this part of the study, focusing on lipids that ionize in the negative ionization mode, the MS was auto-tuned with an LPC, PC, PE, PS, and PG. The rationale was determined based on observations that changes in lipid structure can result in differential ionization efficiencies^{4,5}. This experiment was performed to find the parameters that balanced TL and SV from the initial manual tuning results and would provide low ISF of LPLs, SMs and PCs. Tuning with a PG or a PE produced high TL and SV parameters (SV = 46, TL = 185) both of which led to ISF in the manual tuning studies (**Supplemental**

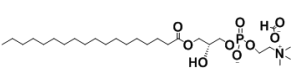
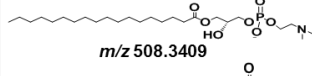
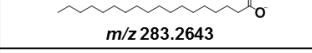
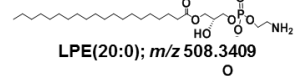
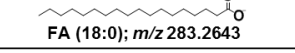
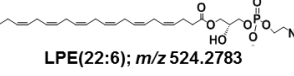
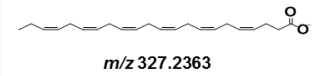
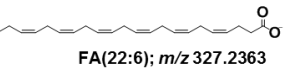
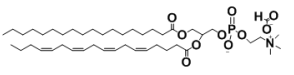
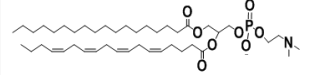
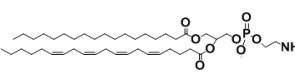
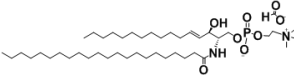
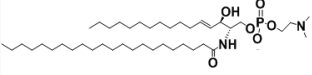
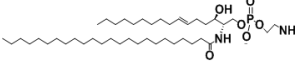
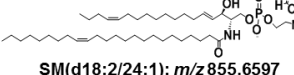
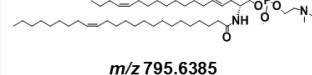
Figure 2) described above, as well as in our general method). Tuning with either a PC or a PS produced SV below 30, but a high TL (above 170), which based on manual assessment exhibited reduced ISF but did not eliminate it. Tuning with an LPC, produced the lowest SV and TL voltages (SV 20 and TL ~140), which produced the lowest ISF in the above experiments, while also maintaining high levels of the molecular ion LPC(19:0) in the manual experiments. We note that the use of an unsaturated phospholipid, when compared to a saturated phospholipid led to slightly lower TL voltages. (Results not shown).

As noted above, the choice of compound used to auto-tune an ESI source can have a dramatic effect on the ionization efficiency of structurally different compounds in a mixture. Moreover, higher voltages can enhance ion yield even though they facilitate fragmentation. It was therefore important to establish whether lowering the SV and TL affected the ionization efficiency of other lipid classes other than choline containing lipids. The ionization efficiency of multiple lipid classes from a human plasma sample was directly assessed (by looking at the ion count) after tuning with the lipids above. We assessed both lipids that fragment in-source (i.e. LPLs, PC and SM), as well as PGs and PIs, which preferentially ionize in the negative mode (**Supplemental Table 4**). For all lipids studied, the differences in parent ion counts were below 5%. Coupled with the data above, these results show that tuning with an LPC provided the best balance for ion transmission of different lipids and low ISF. Therefore, for subsequent experiments, we tuned the MS with an LPC.

Supplemental Table 4:

Lipid	<i>m/z</i>	Ion Count	Ion Count	Ion Count
		Tune LPC (SV 20, TL 140)	Tune PC (SV 26, TL 185)	Tune PG (SV 46, TL 185)
PG(15:0/15:0)	693.4719	1.71E+05	1.56E+05	1.70E+05
LPE(18:2)	476.2804	8.98E+03	6.88E+03	6.56E+03
LPE(20:4)	500.2783	7.27E+03	6.48E+03	4.80E+03
LPC (16:1)	538.3150	8.14E+03	6.69E+03	1.59E+03
LPC(20:4)	588.3332	3.61E+04	2.87E+04	9.24E+03
PE(34:2)	714.5079	4.83E+04	5.66E+04	8.24E+04
PE(36:4)	738.5079	7.49E+04	7.58E+04	1.19E+05
PC(32:0)	778.5620	1.70E+05	1.85E+05	1.93E+05
PC(36:4)	826.5622	2.79E+06	2.84E+06	3.68E+06
PC(17:0/17:0)	806.5917	1.15E+05	1.39E+05	1.32E+05
PI(38:6)	881.5201	2.01E+04	5.32E+03	5.17E+03
PI(38:3)	887.5644	2.41E+05	2.13E+05	2.33E+05
SM(d18:0/16:0)	749.5818	6.64E+04	7.84E+04	5.68E+04
SM(d18:0/18:1)	775.5970	2.14E+05	2.61E+05	2.00E+05

Supplemental Table 4: Tuning the MS with LPC does not reduce ionization efficiency. The ion count of the molecular ion of select lipids observed in negative mode after tuning the ESI source with either an LPC, PC, or PG.

Lipid (Observed m/z)	In-Source Fragment Ion	What In-Source can be Misannotated as
 <p>LPC(18:0); m/z 568.3620</p>	 <p>m/z 508.3409</p>  <p>m/z 283.2643</p>	 <p>LPE(20:0); m/z 508.3409</p>  <p>FA (18:0); m/z 283.2643</p>
 <p>LPE(22:6); m/z 524.2783</p>	 <p>m/z 327.2363</p>	 <p>FA(22:6); m/z 327.2363</p>
 <p>PC(18:0/18:4); m/z 826.5604</p>	 <p>m/z 766.5392</p>	 <p>PE(18:0/20:4); m/z 766.5392</p>
 <p>SM(d16:1/22:0); m/z 803.6284</p>	 <p>m/z 743.6072</p>	 <p>Cer-PE (d16:1/24:0); m/z 743.6072</p>
 <p>SM(d18:2/24:1); m/z 855.6597</p>	 <p>m/z 795.6385</p>	

Supplemental Table 5: Examples of in-source fragmentation of the lipid classes affected by ISF. The first column shows the ions formed from the intact lipids. The second column shows the in-source fragments observed while the third column shows what lipid the in-source fragment can be misannotated. For SMs, the in-source fragments can be misannotated as cer-PE (cer-PEs are not found in humans)⁶ in most cases, the in-source fragment ions do not represent endogenous lipids.

References:

- (1) Bird, S. S.; Marur, V. R.; Sniatynski, M. J.; Greenberg, H. K.; Kristal, B. S. *Analytical Chemistry* **2011**, 83, 6648-6657.
- (2) Bird, S. S.; Marur, V. R.; Sniatynski, M. J.; Greenberg, H. K.; Kristal, B. S. *Analytical Chemistry* **2011**, 83, 940-949.
- (3) Page, J. S.; Kelly, R. T.; Tang, K.; Smith, R. D. *Journal of the American Society for Mass Spectrometry* **2007**, 18, 1582-1590.
- (4) Koivusalo, M.; Haimi, P.; Heikinheimo, L.; Kostinen, R.; Somerharju, P. *Journal of Lipid Research* **2001**, 42, 663-672.
- (5) Gross, R. W.; Han, X. *Chemistry & Biology* **2011**, 18, 284-291.
- (6) Masood, M. A.; Yuan, C.; Acharya, J. K.; Veenstra, T. D.; Blonder, J. *Analytical Biochemistry* **2010**, 400, 259-269.